



Experiment title: Determination of the Fe speciation in cementitious materials using XAFS	Experiment number: EC-487	
Beamline: BM 26A	Date of experiment: from: 9.7.2009 to: 14.7.2009	Date of report: 26.2.2010
Shifts: 15	Local contact(s): Marika Vespa	<i>Received at ESRF:</i>
Names and affiliations of applicants (* indicates experimentalists): R. Daehn*, B. Dilnesa*, E. Wieland*, B. Lothenbach Laboratory for Waste Management, Paul Scherrer Institute, CH-5232 Villigen, Switzerland		

Unhydrated ordinary Portland cement (OPC) is a complex material, which consists mainly of the clinker phases calcium silicates (Ca_3SiO_5 and Ca_2SiO_4), aluminates ($\text{Ca}_3\text{Al}_2\text{O}_6$) and aluminoferrite ($\text{Ca}_4(\text{Fe}_{x-1}\text{Al}_x)_4\text{O}_{10}$), denoted as C_3S , C_2S , C_3A and C_4AF , respectively. Other minerals e.g. calcium sulfate or limestone, are usually also present. In contact with water the hydration process starts, and the clinker phases dissolve slowly and release continuously Ca, Si, Al, Fe(III), SO_4^{2-} and OH^- to solution, which then precipitate as hydrate phases, such as calcium silicate hydrates (C-S-H), AFt phases (e.g. ettringite), AFm phases (e.g. monocarbonate, monosulfate) or other hydrate phases. The Al_2O_3 present in OPC gives rise to the formation of AFm, AFt, hydrogarnet and hydrotalcite. OPC also contains around 4 % of Fe_2O_3 . While the fate of Al during the hydration process is well understood, the Fe speciation, and in particular the chemical nature of the Fe-bearing cement minerals present in the paste, is poorly known. The formation of Fe-silicious hydrogarnets has been reported in some studies while others indicate presence of amorphous Fe-hydroxides or mixed Al-Fe-hydrates. Conclusive identification of the Fe-bearing hydrates in cement pastes using common techniques like XRD, TGA and ESEM is difficult as their signals overlap to a large extent with those of the Al-bearing phases. Therefore, EXAFS was considered to be well suited for Fe speciation studies in cement pastes, as it is an element-specific technique, which allows to overcome the inherent problem of overlapping signals. Fe K-edge EXAFS spectra were collected using synthetic Fe-bearing hydrates and taken as reference spectra for the subsequent analysis of the composite Fe EXAFS spectra recorded in cement pastes.

Important Fe-bearing cement minerals, such as Fe-monocarbonate (Fe-Mc), Fe-ettringite (Fe-Ett), and Fe-silicious hydrogarnet (Fe-Si-Hg) and Fe-hydrotalcite (Fe-Hyd), as well as the Fe-bearing clinker minerals, C_4AF and C_2F , and ferrihydrate ($\text{Fe}(\text{OH})_3$), were synthesized and characterized using standard techniques (XRD, TGA). Structural information was obtained from the EXAFS data by performing multishell fits in real space across the first and second shells in the radial structure functions (RSF) (Table 1). RSF (not shown) were obtained by Fourier transforming k^3 -weighted $\chi(k)$ functions (not shown) between 3 and 11 \AA^{-1} . EXAFS data reduction was performed using the ATHENA/ARTEMIS software package. Theoretical scattering paths for the fits were calculated using FEFF 8.20. The structural parameters of the different compounds were found to be consistent with those obtained from XRD.

Cement pastes were prepared by mixing unhydrated cement and water, and let them hydrate up to one year. The composite Fe EXAFS spectra were analysed using principal component analysis in combination with target transformation, which allowed the number of components to be determined. A preliminary data analysis shows that the composite spectra (Fig. 1) can be fitted using up to three components, i.e., C_4AF , $\text{Fe}(\text{OH})_3$ and Fe-Si-Hg. The relative portion of the cement minerals changes with time. The amount of C_4AF decreases within the first day of hydration. The Fe dissolved from C_4AF forms ferrihydrite (amorphous or poorly crystalline $\text{Fe}(\text{OH})_3$), which is reflected in significant changes in the double beat pattern at around 4 - 5 \AA^{-1} and 8 - 9 \AA^{-1} . After 16 hours of hydration, Fe-Si-Hg starts to appear. The formation of Fe-Si-Hg increases and the amount of ferrihydrite decreases, while the portion of C_4AF remains constant. This

indicates that the ferrihydrite initially formed re-precipitates as Fe-Si-Hg in the long term. The slow formation of Fe-Si-Hg at room temperature was confirmed in solubility experiments.

This study reveals that, in the early phase of cement hydration, ferrite is converted into ferrihydrite. In the long run, however, ferrihydrite is unstable and converts into Fe-siliceous hydrogarnet, which is thermodynamically stable. This finding is essential in connection with future investigations on cement-water interaction with a view to predicting the long-term properties of cementitious materials and assessments made in conjunction with the safe disposal of radioactive and hazardous wastes.

Table 1: Structural information obtained from Fe K-edge data analysis of references

Phases	Atomic pair	N	$\sigma(\text{\AA}^2)$	R(\AA)	R-Factor(%)
C ₄ AF	Fe-O	3.9	0.009	1.95	2.0
	Fe-Ca	5.1	0.011	3.12	
	Fe-Fe	5.0	0.007	3.60	
	Fe-Al	4.8	0.004	3.59	
Fe(OH) ₃	Fe-O	6.0 ⁺	0.012	2.01	3.3
	Fe-Fe	4.0 ⁺	0.012	3.04	
	Fe-Fe	4.0 ⁺	0.013	3.41	
Fe-monocarbonate	Fe-O	6.4	0.006	2.02	5.0
	Fe-Ca	5.8	0.008	3.47	
Fe-ettringite	Fe-O	5.4	0.004	2.03	2.5
	Fe-Ca	5.1	0.01	3.52	
Fe-hydroxalite	Fe-O	5.7	0.003	2.03	1.5
	Fe-Mg	6.0 ⁺	0.005	3.13	
Fe-siliceous hydrogarnet	Fe-O	6.0 ⁺	0.009	2.01	3.7
	Fe-Si	6.0 ⁺	0.005	3.39	
	Fe-Ca	6.0 ⁺	0.007	3.46	

N: Coordination number of the neighboring atom (uncertainty $\pm 20\%$)

R: Distance to the neighboring atom (uncertainty $\pm 0.02 \text{ \AA}$)

σ : Debye-Waller factor

+ : fixed parameters during fitting

* : values from Al-containing phases

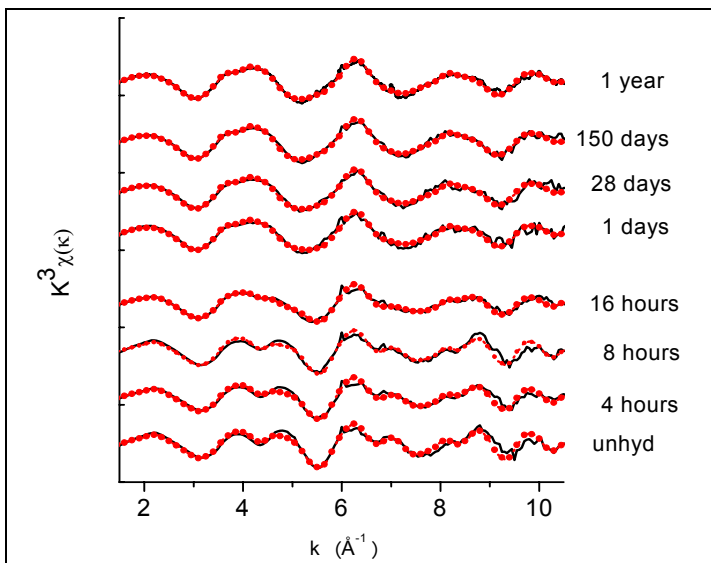


Fig. 1: EXAFS spectra of hydrated OPC at different hydration times (line: experimental data; dots: modelled data)

Table 2: Relative portion of Fe-bearing phases in OPC hydrated at 20 °C obtained from LC fitting

Hydration time	C ₄ AF	Fe(OH) ₃	Fe-Si-Hg	R-factor*
Unhydrated	1			0.18
4 hours	0.59	0.42		0.14
8 hours	0.67	0.33		0.14
16 hours	0.38	0.43	0.19	0.1
1 day	0.29	0.19	0.52	0.14
28 days	0.26	0.15	0.59	0.1
150 days	0.22	0.15	0.63	0.06
1 year	0.26	0.13	0.62	0.05

* R-factor: Goodness of fit indicator or measure of the residual, respectively. Decreases with increasing agreement between fit and experimental data.